Pion charge exchange on deuterium

J.-P. Dedonder
GMPIB, Université Paris 7–Denis Diderot, 2 Place Jussieu, F75251 Paris cedex 05, France

W. R. Gibbs
Department of Physics, New Mexico State University, Las Cruces, New Mexico 88003, USA
(Received 9 December 2003; published 28 May 2004)

We investigate quantum corrections to a classical intranuclear cascade simulation of pion single charge exchange on the deuteron. In order to separate various effects, the orders of scattering need to be distinguished and, to that end, we develop signals for each order of scattering corresponding to quasifree conditions. Quantum corrections are evaluated for double scattering and are found to be large. Global agreement with the data is good.

DOI: 10.1103/PhysRevC.69.054611 PACS number(s): 25.80.Gn, 25.10.+s, 24.10.Lx

I. INTRODUCTION

The solution of the many-body Schrödinger equation for scattering problems is difficult indeed. For this reason quantum mechanical reaction calculations are often replaced with their classical analogs. The replacement of the quantum problem by the classical one was first suggested by Serber [1]. He observed that the early data seemed to be consistent with a simple cascade of collisions within a Fermi gas model of the nucleus. This idea was followed by a long list of developing codes (see Refs. [2–16]).

For heavy-ion reactions the final state is very complicated, and the cascade calculation became one of the few tools available to predict results. The relativistic quantum molecular dynamics (RQMD) approach [8] and the Liège code [9] provide two standard calculational techniques for treating intermediate energy heavy ion reactions. The code from Valencia [10] is capable of treating proton and pion projectiles. New approaches include a code developed by Li *et al.* [11] using a set of coupled transport equations and a cascade model developed with relativistic heavy-ion collisions in mind, the ARC (a relativistic cascade) code [12].

Almost all of these models rely on the treatment of the scattering from the point of view of classical probabilities with each scattering being treated independently. Of course we know that there are phases arising from quantum mechanics which should enter into the calculation of the total probability.

If one wanted to perform a fully quantum mechanical cascade one possibility might be to consider all possible results arising from the initial conditions and then calculate the quantum mechanical probability of each event. These probabilities would then be used as weights. This would be an extremely inefficient procedure, however, since the dominant fraction of the events, if chosen completely randomly, would occur with very small probability and most of the calculational time would be wasted. A far more efficient procedure would be to choose the events according to some approximate (well defined) probabilistic rule and then correct the approximate rule by taking for the weight of the event the ratio of the probabilities. This is a standard technique in Monte Carlo procedures known as "importance sampling." The approximate event generator must have the property that it can be sampled and that the probability for a given event can be calculated. Of course, the full calculation will be more efficient if the event generator gives results close to the "correct" answer. For this event generator we will use the classical simulation mentioned above. It is known to give good results for simple reactions such as quasielastic scattering. Deviations from the model are also seen, and it is never sure if these discrepancies should be ascribed to new physics or to the fact that the model is purely classical. Because of its simplicity we have chosen the $\pi^+ + d \rightarrow pp\pi^0$ reaction to investigate some quantum corrections.

To elucidate, to the extent possible, the role and magnitude of the quantum corrections, we have been led to explore the role of various parameters (counter size, lower momentum cuts, absorption parameters, etc.) in relation to either the data or the model.

II. DATA

For the case of single charge exchange on the deuteron, there exist fairly complete data [13] on the cross section with a coincidence between the two final protons such that the final state was entirely determined. The coincidences were between pairs of counters on opposite sides of the beam at 228 and 294 MeV so that the reaction took place in a plane. The counter positions are at 20°, 45°, 60°, and 125° on each side of the beam. This would seem to give 16 pairs but all coincidences are not possible. Removing the $(20°,-20°)$, $(60°,-125°)$, $(125°,-60°)$, and $(125°,-125°)$ cases, there remain 12 angle pairs. By convention, the momentum distribution displayed will be that of the counter corresponding to the first element of the angle pair.

The coincidence requirement opens up new possibilities for analyzing the data. The quantum correction that we consider is the one due to quantum vs classical double scattering. The data of Tacik *et al.* [13] present the opportunity to explore its nature. One might think that the double scattering contribution to single charge exchange on the deuteron is small, and that is, in general, true. However, in the cases in which just one charge exchange on the neutron takes place

(without a scattering from the other nucleon), the spectator proton has very low momentum in the final state due to the low Fermi momentum of the deuteron. In most experiments (in particular the one we shall consider here [13]), the two protons are detected with a minimum momentum. Under these conditions the double and higher scattering contributions are the most important.

This positive feature is balanced by the fact that the acceptance of the experimental system must be understood. Since the spectrum of one proton was measured in coincidence with the second proton the threshold on the second detector is important.

The data show a smooth variation as a function the counter pair position as well as a function of incident pion energy. However there are very strong, narrow peaks in the momentum spectra which are perhaps surprising. We shall argue that these peaks are normal kinematic features and can, to some extent, serve as indicators of orders of scattering. We need to characterize the data in terms of the multiple scattering components since the relative weights of each order are different at 228 and 294 MeV.

In the treatment of these data we first run a cascade code to generate an event file with charge exchange events. This file is then analyzed with appropriate threshold cuts, selection of the number of scatterings, etc. After some studies attempting to match the experimental thresholds we decided to use a standard momentum threshold of 226 MeV/c for all of the cases. The counters were taken to have an extension of 5° in the θ sense and the back-to-back condition was enforced by requiring that $\cos\Delta\phi \leqslant -0.99$, where $\Delta\phi$ is the difference in azimuthal angles for the two protons.

III. CLASSICAL CODE

The present INC (intranuclear cascade) code was originally developed to treat moderate-energy antiproton annihilation in nuclei and has been applied to that end several times [14–18]. However, the annihilation of an antiproton leads to pions (or at least it is so treated by the model) and so the history of pions in the energy range below, and of the order of, 1 GeV is essential to the calculation of energy deposition. Of particular importance for the thermalization of the nuclear matter are pion absorption and production. For this reason the code needed to be checked against reactions initiated by pion beams [19]. Calculations have been done to compare with data on antiproton annihilation of $5-10$ GeV antiprotons on several nuclei [20]. Considerable success has been obtained in predicting the rapidity distributions of strange particles produced in antiproton reactions [18]. The question of pion absorption and comparison with data has been addressed [21] and the code has been used for the comparison with inclusive data [22]. It was quite successful in describing the overall spectrum although there is a problem with the number of final pions in the region of the delta resonance.

A description of the basic features of the pion version of the code can be found in Ref. [23] where pion double charge exchange on ^{4}He was treated with a quantum correction for final state interaction for the (unobserved) nucleon pair on which the two charge exchanges took place. This was an important correction since, for high-energy final pions, these two nucleons often have low relative energies. In the present case the two final nucleons cannot have low relative energies (because the counter pairs require a substantial separation in angle) so this final state interaction correction was not included.

As can be seen in the above mentioned descriptions, the absorption is controlled by a parameter which expresses the probability that an absorption takes place when it is permitted by conservation laws. In the present work we varied this parameter to fit the experimental absorption cross sections [24]. Even large variations of the cross-section (a factor of 2) led to variations in the magnitude of the charge exchange cross sections of at most of the order of 20–30 % with no major change in the shape of the spectra.

The first problem to be approached in attempting to make a classical solution to the many-body scattering system act as a simulation of the quantum system is the realization of the initial density of particles in the bound target. While one can choose the coordinate positions appropriately, the distribution of momenta of the particles also needs to be taken to match the quantum case. The technique for the construction of a nucleus with A nucleons is given in Ref. [23].

For the case of the deuteron a direct sampling method can be used to take the spatial distribution directly from a probability density. For the radial density we have taken that of the solution with a one-pion-exchange potential [25–28].

Since we intend to have the two nucleons propagate under the action of a potential, once the position of an initial nucleon is established the kinetic energy is fixed by the relation

$$T(r) + V(r) = E, \tag{1}$$

where T is the kinetic energy of the particle and V is the potential chosen. Once a value of r is chosen then a value of the kinetic energy (and hence of momentum) is fixed. Since (as we will see shortly) the coincidence requirement leads to delta functions for the momentum distributions for double scattering in the absence of Fermi motion in the deuteron, it is important that the distribution of this quantity be realistic.

If the potential in this equation is chosen to be the same as that used in the quantum mechanical problem to provide a solution giving the density, in general the distribution of the momenta obtained from the classical procedure just outlined will give a (very) different distribution of momenta from the one obtained from the square of the momentum space wave function derived from the solution of the quantum problem. In particular, the quantum solution gives a distribution of momenta which has support to infinity, whereas the classical solution, because of the fact that a typical potential used in the solution of the nucleon-nucleon problem has a maximum depth, has a cutoff at a finite value. This cutoff comes at a point well within the range of interest of momenta so that the resulting momentum distribution is far from realistic.

This problem can be solved (at an expense as we shall see) by choosing the potential such that the momentum distribution is correct if the radial density is the one desired. In the present case, we have taken the binding energy of the

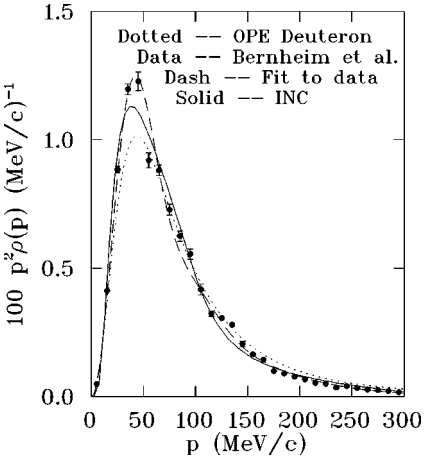

FIG. 1. Comparison of the measurements of Fermi momenta by Bernheim *et al.* [29] with a fit to the data (dashed line) and the result of the INC (solid line) using the potential derived in the text and shown in Fig. 2. Also shown is the square of the momentum wave function of the one-pion-exchange deuteron (dotted).

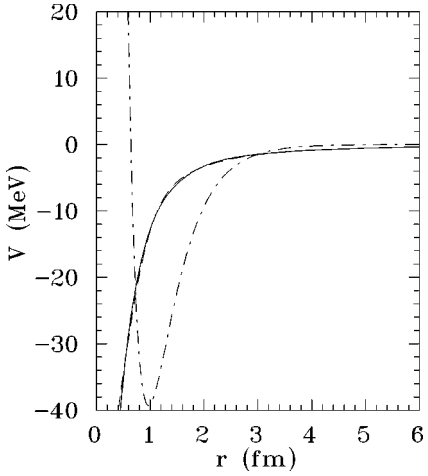

FIG. 2. The potential obtained as described in the text. The solid line is the potential directly from the procedure and the dashed line shows the fit used in the cascade code. The dash-dotted line shows the Malfliet-Tjon [30] potential as modified in [28].

deuteron to be zero so that the kinetic energy is equal to the negative of the potential.

To find the potential which will make these two distributions compatible in the classical sense, we first transform the momentum distribution to a distribution of kinetic energies. The momentum distribution used in this case is taken from a fit to the data of Bernheim *et al.* [29] where the data and the fit are shown in Fig. 1.

Given this distribution, the condition that the kinetic energy distribution $g(T)$ be obtained from a given radial distribution $\rho(r)$ is

$$\rho(r)dr = g(T)dT \tag{2}$$

for which the integrated form (taking account of the proper limits to give the boundary conditions) is

$$F(r) \equiv \int_r^\infty \rho(r)dr = \int_0^T g(T)dT \equiv G(T). \tag{3}$$

To obtain the desired solution the functions $F(r)$ and $G(T)$ are tabulated numerically and then the numerical inversion

$$T(r) = G^{-1}[F(r)] \tag{4}$$

is made. The potential is then identified with the negative of the kinetic energy. The numerical inversion procedure introduces some error but is stable except for very small values of r, where the numerical procedure limits to a constant potential, whereas the true result goes to infinity. A fit is then made to the potential which follows the potential in the region where it is well determined. In general the procedure works well and the resultant momentum distribution from the simulation is shown in Fig. 1 compared with the input distribution. The agreement is good but not perfect.

The resulting potential is shown in Fig. 2. It is seen that it has only a cursory resemblance to a semirealistic *NN* potential at large r and is completely different at small r where it lacks the repulsive hard core. This potential is the price paid for being able to have correct spatial and momentum distributions with conservation of energy. For double scattering or higher this potential is not very important since the nucleons have high energies and are little affected by the final state interaction between the two nucleons.

For single scattering, however, where the Fermi momentum (after final state interaction) must be detected in one of the pair of counters, the error can be substantial. Since only the tail of the Fermi momentum distribution has large enough values of momentum to be observed in the detectors, the exact values of the momentum in the tail is crucial. For a number of cases the single scattering plays a small role while for others it contributes in certain parts of the spectrum in ways that might not be imagined without some reflection.

Since we know the initial distribution and we can select the events with single scattering in the calculation and accumulate the distributions of the final proton momenta, the effect of this potential in the final state can be observed. Figure 3 shows such a comparison for four angle pairs. The curves have been normalized to the same integral values. It is seen that the momenta for the case of the forward angle counters have been shifted to lower values as expected from the above arguments. In other cases the distribution is very similar to the starting distribution or increased at high momenta. The largest angle counters show a double peaked structure.

IV. SINGLE, DOUBLE, AND TRIPLE SCATTERING

While the quasifree single scattering peak has been known for a long time, it is interesting that in a coincidence experiment one can expect peaks from quasifree double and triple scattering. Since peaks in spectra are sometimes interpreted as particle masses, one should be aware of the possible presence of such peaks to avoid misinterpretations that could arise. Scattering is carried only to fourth order, i.e., after the pion has scattered four times it is not allowed to interact. Thus, what we call quadruple scattering really represents all of the rest of the scatterings which would have

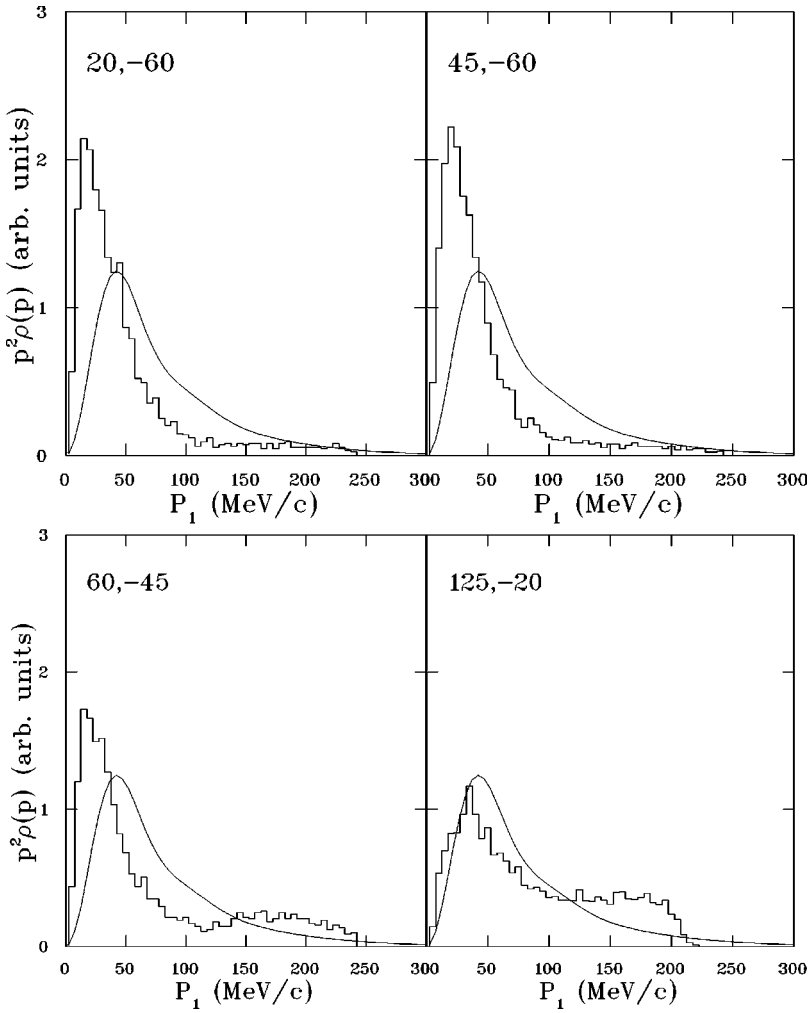

FIG. 3. Comparison of the observed final momentum of the unstruck particle in single scattering events with the initial Fermi momentum (its initial momentum before interaction with the potential).

occurred as well. We are not able to give an analytical discussion of this higher order but we will treat the first three orders.

A. Single scattering

The quasifree scattering peak is well known in measurements in which a single particle is observed and, indeed, appears prominently in many cases. It corresponds to a free nucleon at rest being struck. Since the Fermi momentum distribution typically peaks at zero (or low) momentum, a peak in the final momentum distribution is observed at the value of momentum appropriate for free scattering. In addition there is a distribution of counts on either side with the extent of the wings depending on the Fermi momenta.

In the present coincidence experiment, where for the case of single scattering a substantial Fermi momentum is needed for the observation of the spectator proton, the maximum of the quasifree peak is explicitly excluded. The most one might expect to see is one or both of the wings of the distribution. This effect can lead to rather unexpected contributions to the spectrum.

Figure 4 shows results for single scattering. The dotted curve shows the distribution without any thresholds for the counters, and the quasifree peak is clearly seen. The solid curve displays the result with the threshold cuts in place and one sees that most of the single scattering is eliminated by the cuts. In some cases a remnant of the single scattering is left. Interesting are the cases of the angle pairs $(45°,-45°)$ and $(60°,-20°)$ where the quasifree peak is in the center of the spectrum and only the tails of the distribution remain after the cut resulting in peaks at high and low momenta, with precisely the opposite shape to the original spectrum before the cuts. Clearly, it is difficult to be sure of the strength of these peaks since they depend on the values of the cuts and, especially, on the final state interaction potential. In these two cases, since the momentum distribution has been modified only slightly by the final state interaction, one may expect that the predictions are at least qualitatively correct.

The remnants after cuts shown in Fig. 4 for 294 MeV are among the largest for that energy. The remaining single scattering cross sections at 228 MeV are large, not only in the case of the counter pairs shown but in the pairs $(20°,-45°)$ and $(45°,-20°)$ and to a lesser extent for the pairs $(45°,-60°)$ and $(60°,-45°)$. For the $(20°,-60°)$ angle pair the final momentum for the quasifree peak is clearly visible without cuts but mostly eliminated with them. The effect of the cuts is rather different at 228 MeV and 294 MeV.

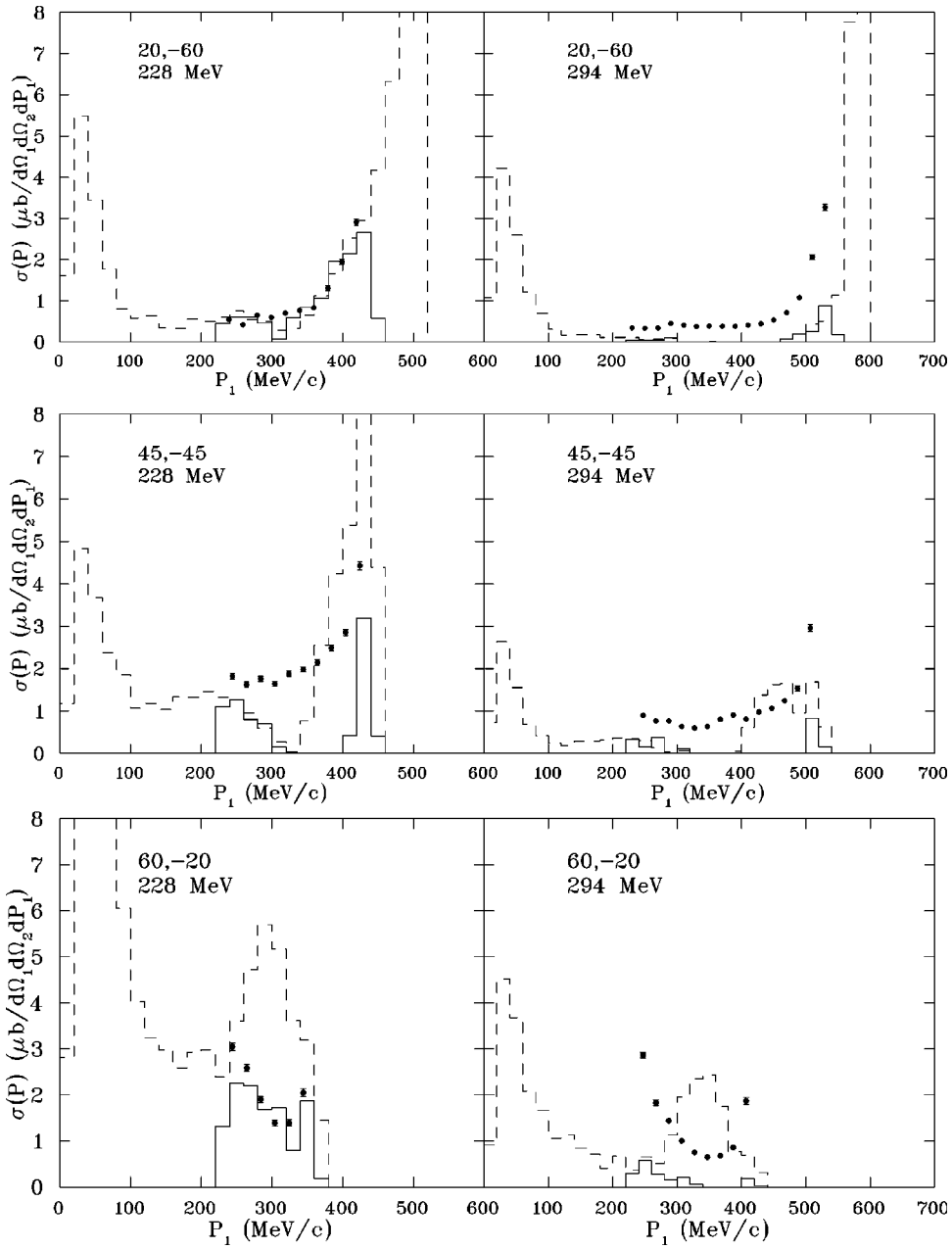

FIG. 4. Single scattering with and without cuts at 228 and 294 MeV. The data points shown in this figure and all of the figures to follow are from [13].

B. Double scattering

We now discuss the existence of quasifree double scattering peaks where each of the two particles will receive a substantial momentum from the scattering process. For this reason in this study we limit ourselves to the case of zero Fermi momentum. By specifying the angle of the outgoing (first) nucleon, with the incident pion momentum known, the kinematics of the reaction are expressed by

$$\mathbf{k}_\pi = \mathbf{k}_1 + \mathbf{k}, \tag{5}$$

where $\mathbf{k}_1$ is the final energy of the first struck nucleon and $\mathbf{k}$ is the pion momentum after the first scattering. Equating the total laboratory energy before and after scattering, we have

$$E = \omega + M = \sqrt{\mu^2 + (\mathbf{k}_\pi - \mathbf{k}_1)^2} + \sqrt{M^2 + k_1^2}$$
$$= \sqrt{\mu^2 + k_\pi^2 + k_1^2 - 2k_\pi k_1 x} + \sqrt{M^2 + k_1^2}, \tag{6}$$

where x is the cosine of the angle between the incident pion direction and $\mathbf{k}_1$. Solving this equation for $|\mathbf{k}_1|$, we have

$$|\mathbf{k}_1| = k_1 = \frac{2Mk_\pi x}{E - k_\pi^2 x^2/E}. \tag{7}$$

Since the final pion momentum from the first scattering is known, it can be used as input for the second scattering, and, with the direction of the final nucleon fixed by the experimental conditions, all angles and energies are again known. We can apply the same formula to find

TABLE I. Expected peaks from quasifree double scattering for a pion incident energy of 294 MeV. The numbers are for the position of peaks expected in the first counter of the pair. The first number corresponds to the case where the first struck nucleon was detected in this counter and the second number corresponds to the case where the second scattered nucleon was detected in the first member of the counter pair. In the pairs in which one of the counters is at 125°, only one value is possible since the first scattering cannot lead to a particle recoiling at greater than 90° (without Fermi motion).

Angle pair	20, 125	20, 60	20, 45	
Peak position(s) (MeV/c)	573	573 507	573 316	
Angle pair	45, 125	45, 60	45, 45	45, 20
Peak position(s) (MeV/c)	415	415 557	415 447	415 75
Angle pair		60, 60	60, 45	60, 20
Peak positions (MeV/c)		287 529	287 486	287 165
Angle pair			125, 45	125, 20
Peak position (MeV/c)			259	376

$$k_2 = \frac{2Mky}{E' - k^2 y^2 / E'}, \tag{8}$$

where $E' = \sqrt{k^2 + \mu^2} + M$ and y is the cosine of the angle between $\mathbf{k}$ and $\mathbf{k}_2$.

Thus, for a given angle pair there are two momenta (each in a different counter) where one might expect to observe a peak. Since the first scattering must lead to the recoil of the nucleon in the forward direction, when one counter at 125° is involved there is only one value possible corresponding to the scattering to the forward counter first. Tables I and II give the peak position expected at 294 and 228 MeV, respectively.

Figure 5 compares calculations with and without Fermi momentum for double and total scattering. They are made including the quantum correction to be discussed in the next section. It is seen that peaks do indeed come where predicted by the above considerations (shown as triangles in the figure). Fermi motion and higher order scatterings tend to blur and hide them but they are often visible in the final result.

C. Triple scattering

In this case (perhaps remarkably) one also has regions of strength in the quasifree process. The reason for the existence of structure is a Jacobian peak introduced by a transformation discussed in the following. If we assume that the entire triple scattering remains in a plane, then for a given value of the recoil angle for the initial scattering, θ_1^i, for a fixed θ_2 all kinematics are defined. The probability of such an event will be given in terms of a product of the three scattering cross sections involved. Performing the transformation from the distribution in $z = \cos\theta_1^i$ to the distribution in final momenta $k_1(z)$ (the momentum of the first nucleon *after* the *second* scattering), the momentum distribution is given by

$$\frac{dP}{dk_1} = \frac{dP}{dz} \Big/ \left| \frac{dk_1}{dz} \right|, \tag{9}$$

where the quantity dP/dk_1 is the probability of the triple scattering taking place for a given z. dk_1/dz typically has a zero in the range of interest. This zero occurs at the maximum energy possible for triple scattering, which, in fact, coincides with the maximum energy possible for the reaction (regardless of the number of scatterings). Triple scattering is the first order in which this maximum momentum can be reached. This peak will have the same form for any value of Fermi momentum and hence is not broadened by the motion of the nucleon. Since the measurement is a coincidence cross section, one expects a companion peak in the second counter at the energy of the second scattering which corresponds to the Jacobian peak. While the Jacobian peak is clearly seen in the experimental results the companion peak is usually much broader and generally not visible. It is worthwhile to note that the counter size can influence what is seen since there is

TABLE II. Expected peaks from quasifree double scattering for a pion incident energy of 228 MeV. See Table I for an explanation of the entries.

Angle pair	20, 125	20, 60	20, 45	
Peak position(s) (MeV/c)	488	488 427	488 260	
Angle pair	45, 125	45, 60	45, 45	45, 20
Peak position(s) (MeV/c)	357	357 476	357 378	357 54
Angle pair		60, 60	60, 45	60, 20
Peak positions (MeV/c)		249 458	249 416	249 135
Angle pair			125, 45	125, 20
Peak position (MeV/c)			241	334

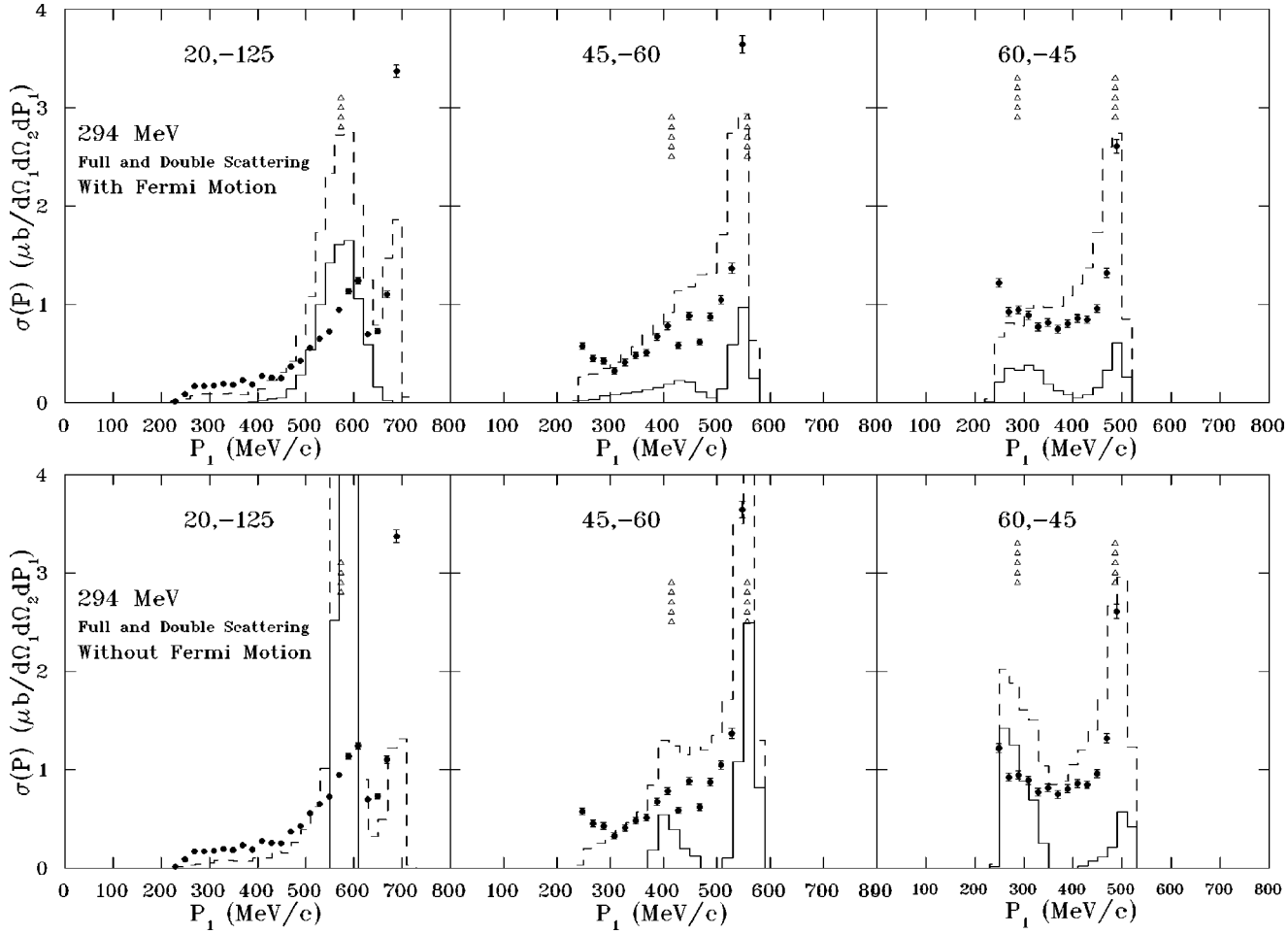

FIG. 5. Total and double scattering with and without Fermi motion at 294 MeV. The solid line represents the contribution of double scattering and the dashed line gives the total. Both calculations were made without absorption.

a true singularity in these peaks. Table III gives the positions of these Jacobian peaks and the companion peak.

Figure 6 gives the final momenta of the two nucleons as a function of the (assumed in plane) scattering angle in the first scattering for the angle pairs $(20°, -125°)$ and $(125°, -20°)$. It is seen that the momentum of the particle in the second counter also has a maximum (and hence also a Jacobian peak) for the case $(125°, -20°)$. For the conjugate pair, $(20°, -125°)$ the case is not realized for the peak of the second momentum. However, this second Jacobian peak in the 20° counter means that there should be two sharp peaks with no Fermi momentum. When Fermi momentum is included in the problem the peak in the interior of the distribution will be broadened but that at the maximum of momentum will not.

Figure 7 shows results of the INC calculation with a very small Fermi momentum. It is seen that the peaks match the predictions (marked with the triangles). While the companion peak to the Jacobian is normally broad (see pair 45°, −60°), we see that, indeed, the angle pair $(20°, -125°)$ is an exception with the second peak being also narrow. There is some broadening of the peaks due to the finite size taken for the counters in the analysis of the events coming from the INC.

V. QUANTUM CORRECTIONS

In this section we discuss the quantum corrections that we apply for the double scattering only. We will treat spin, space, and isospin in turn, starting with the general form of the operator in spin space.

A. General form

In order to calculate the ratio of the quantum double scattering cross section to the classical version we must evaluate the double scattering amplitude, which can be expressed as

$$A_{ds}(\mathbf{k}_\pi, \mathbf{k}'_\pi; r_1, r_2) = \frac{1}{2\pi^2} \int d\mathbf{q} \frac{e^{-i\mathbf{k}'_\pi \cdot r_2} f(\mathbf{q}, \mathbf{k}'_\pi) e^{i\mathbf{q}\cdot(\mathbf{r}_2 - \mathbf{r}_1)} f(\mathbf{k}_\pi, \mathbf{q}) e^{i\mathbf{k}_\pi \cdot \mathbf{r}_1}}{q^2 - \kappa^2 - i\epsilon} \tag{10}$$

$$= \frac{e^{-i(\mathbf{k}'_\pi \cdot \mathbf{r}_2 - \mathbf{k}_\pi \cdot \mathbf{r}_1)}}{2\pi^2} \int d\mathbf{q} \frac{f(\mathbf{q}, \mathbf{k}'_\pi) e^{i\mathbf{q}\cdot\mathbf{r}} f(\mathbf{k}_\pi, \mathbf{q})}{q^2 - \kappa^2 - i\epsilon}. \tag{11}$$

Following the technique of Ref. [31] and including plane wave functions for the nucleon final states, we can express

TABLE III. Expected peaks in triple scattering at 294 and 228 MeV based on the position of the Jacobian singularity. Both entries at a given energy correspond to the momentum in the first member of the angle pair.

	294 MeV		228 MeV	
Angle Pair	k_1(MeV/c)	k_2(MeV/c)	k_1(MeV/c)	k_2(MeV/c)
20, −125	696	606	598	508
45, −125	493	419	440	379
20, −60	585	237	498	199
45, −60	557	336	477	285
60, −60	551	402	475	343
20, −45	576	144	490	117
45, −45	517	227	441	191
60, −45	499	286	428	239
125, −45	259	191	244	189
45, −20	462	38	394	28
60, −20	419	83	358	66
125, −20	377	287	335	252

the amplitude for a fixed position of the two nucleons as an operator on a single function $g(r)$.

$$e^{i(\mathbf{k}_1\cdot\mathbf{r}_1+\mathbf{k}_2\cdot\mathbf{r}_2-\mathbf{k}_\pi\cdot\mathbf{r}_1+\mathbf{k}'_\pi\cdot\mathbf{r}_2)}A_{ds} = (A_1 + B_1\mathbf{q}\cdot\mathbf{k}_\pi + C_1\sigma_1\cdot\mathbf{q}\times\mathbf{k}_\pi) \times(A_2 + B_2\mathbf{k}'_\pi\cdot\mathbf{q} + C_2\sigma_2\cdot\mathbf{k}'_\pi\times\mathbf{q}) \times g(r), \quad (12)$$

where $\mathbf{q}$ is to be interpreted as $-i\boldsymbol{\nabla}$. Here the constants A, B, and C are determined from pion-nucleon phase shifts and correspond to the two processes possible: π^+ elastic scattering on the proton followed by charge exchange on the neutron or charge exchange on the neutron followed by π^0 elastic scattering on the proton. The phase factor on the left could be ignored in some cases but we need to keep it here since we wish to consider the coherence of this scattering (nucleon 1 followed by nucleon 2) with the reverse order.

The function $g(r)$ is given by

$$g(r) = \frac{e^{i\kappa r} - e^{-\alpha r}}{r} - \frac{(\kappa^2+\alpha^2)}{2\alpha}e^{-\alpha r}, \quad (13)$$

where we have taken

$$v(q) = \frac{\alpha^2+\kappa^2}{\alpha^2+q^2}, \quad (14)$$

κ is the momentum of the intermediate propagating pion, and α is the range of the form factor (taken as 4 fm^{-1} here).

We consider the transformations of the radius vectors according to

$$\mathbf{r}_1 = \mathbf{R} + \frac{\mathbf{r}}{2}, \quad \mathbf{r}_2 = \mathbf{R} - \frac{\mathbf{r}}{2}.$$

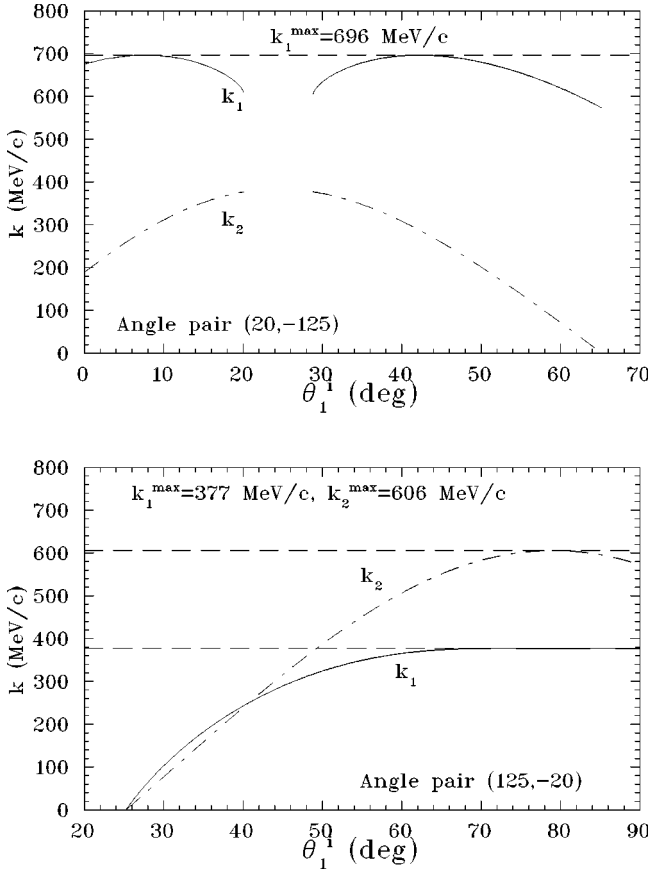

FIG. 6. Momenta for triple scattering at 294 MeV. The momentum k_1 is the one measured in the 20° counter and k_2 that measured in the 125° counter.

We see that we have terms with no, one, and two derivatives. Since $\boldsymbol{\nabla}g(r)=\hat{\mathbf{r}}g'(r)=\mathbf{r}g'(r)/r$ we can make a simple replacement in the terms with one derivative. For the terms with two derivatives a second term appears which corresponds to the operation of the derivative on the factor $\mathbf{r}$. Thus we can expand Eq. (12) as

$$\begin{aligned} &e^{i(\mathbf{k}_1\cdot\mathbf{r}_1+\mathbf{k}_2\cdot\mathbf{r}_2-\mathbf{k}_\pi\cdot\mathbf{r}_1+\mathbf{k}'_\pi\cdot\mathbf{r}_2)}A_{ds} \\ &\quad = A_1A_2g(r) + (A_1B_2\mathbf{k}'_\pi\cdot\mathbf{q} + A_2B_1\mathbf{q}\cdot\mathbf{k}_\pi)g(r) \\ &\qquad + (B_1B_2\mathbf{q}\cdot\mathbf{k}_\pi\mathbf{k}'_\pi\cdot\mathbf{q})g(r) + (A_1C_2\sigma_2\cdot\mathbf{k}'_\pi\times\mathbf{q} \\ &\qquad + A_2C_1\sigma_1\cdot\mathbf{q}\times\mathbf{k}_\pi)g(r) + (B_1C_2\mathbf{q}\cdot\mathbf{k}_\pi\sigma_2\cdot\mathbf{k}'_\pi\times\mathbf{q} \\ &\qquad + B_2C_1\mathbf{k}'_\pi\cdot\mathbf{q}\sigma_1\cdot\mathbf{q}\times\mathbf{k}_\pi)g(r) + (C_1C_2\sigma_1\cdot\mathbf{q} \\ &\qquad \times\mathbf{k}_\pi\sigma_2\cdot\mathbf{k}'_\pi\times\mathbf{q})g(r), \end{aligned} \quad (15)$$

where we have separated the terms according to the number of derivatives and the number of occurrences of the spin operators. Performing the operations we can write (still as an operator in spin space)

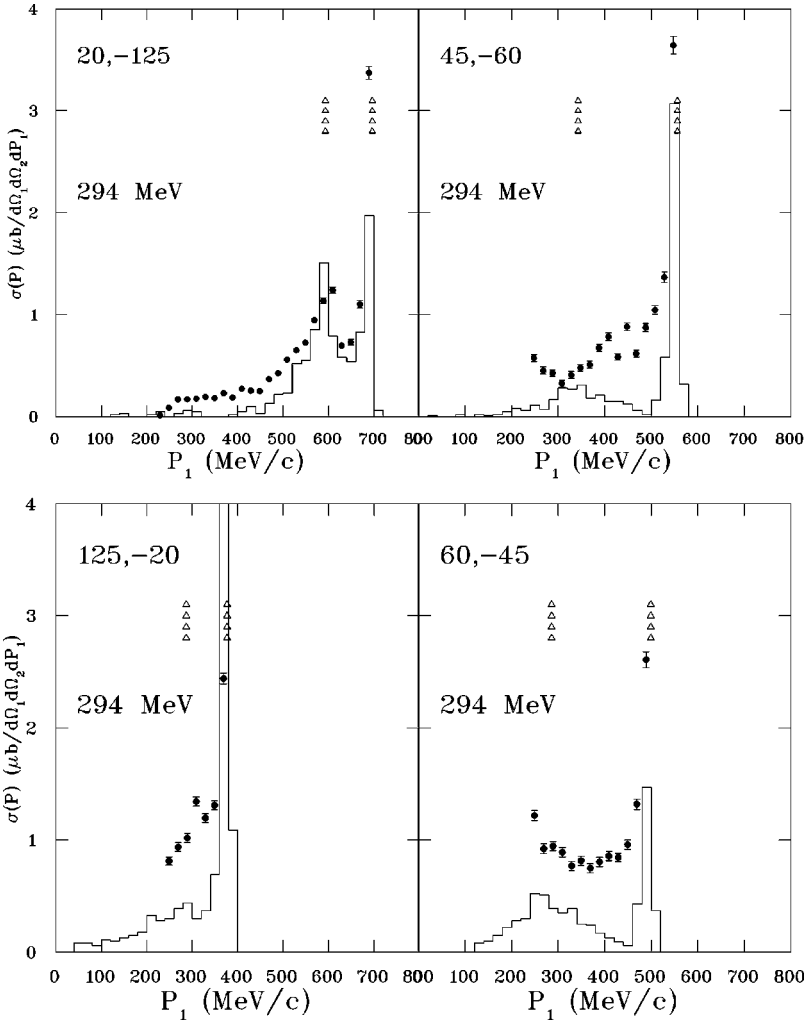

FIG. 7. Triple scattering without cuts, with absorption, and with a small Fermi momentum at 294 MeV to show the kinematic effects of the Jacobian peaks.

$$e^{i(\mathbf{k}_1\cdot\mathbf{r}_1+\mathbf{k}_2\cdot\mathbf{r}_2-\mathbf{k}_\pi\cdot\mathbf{r}_1+\mathbf{k}'_\pi\cdot\mathbf{r}_2)}A_{ds} = A_1A_2g(r) - i(A_1B_2\mathbf{k}'_\pi\cdot\hat{\mathbf{r}} + A_2B_1\hat{\mathbf{r}}\cdot\mathbf{k}_\pi)g'(r) - B_1B_2\hat{\mathbf{r}}\cdot\mathbf{k}_\pi\mathbf{k}'_\pi\cdot\hat{\mathbf{r}}g^-(r) - B_1B_2\mathbf{k}_\pi\cdot\mathbf{k}'_\pi\frac{g'(r)}{r}$$
$$- i(A_1C_2\sigma_2\cdot\mathbf{k}'_\pi\times\hat{\mathbf{r}} + A_2C_1\sigma_1\cdot\hat{\mathbf{r}}\times\mathbf{k}_\pi)g'(r) - (B_1C_2\hat{\mathbf{r}}\cdot\mathbf{k}_\pi\sigma_2\cdot\mathbf{k}'_\pi\times\hat{\mathbf{r}} + B_2C_1\mathbf{k}'_\pi\cdot\hat{\mathbf{r}}\sigma_1\cdot\hat{\mathbf{r}}\mathbf{k}_\pi)g^-(r)$$
$$- (B_1C_2\sigma_2\cdot\mathbf{k}'_\pi\times\mathbf{k}_\pi + B_2C_1\sigma_1\cdot\mathbf{k}'_\pi\times\mathbf{k}_\pi)\frac{g'(r)}{r} - C_1C_2\Bigg[(\sigma_1\cdot\hat{\mathbf{r}}\times\mathbf{k}_\pi\sigma_2\cdot\mathbf{k}'_\pi\times\hat{\mathbf{r}})g^-(r)$$
$$+ (\sigma_1\cdot\mathbf{k}'_\pi\sigma_2\cdot\mathbf{k}_\pi - \sigma_1\cdot\sigma_2\mathbf{k}_\pi\cdot\mathbf{k}'_\pi)\frac{g'(r)}{r}\Bigg], \tag{16}$$

where $g^-(r)\equiv g''(r)-g'/r$.

Terms proportional to $g'(r)/r$ are "quantum" in origin and fall off as $1/r^2$ for large distances. For large values of r also

$$g(r)\to\frac{e^{i\kappa r}}{r},\quad g''(r)\to-\kappa^2\frac{e^{i\kappa r}}{r},\quad g'(r)\to i\kappa\frac{e^{i\kappa r}}{r}.$$

The spin-independent terms will be diagonal in the initial and final states, but we must take the expectation values of the the spin operators for the other terms. We will use the singlet-triplet representation for the present problem since the initial state is a pure triplet. The matrix elements needed for the spin amplitudes are given in Appendix B.

B. Isospin of the deuteron

In order to include the effect the definite isospin of the deuteron we can write the amplitude as

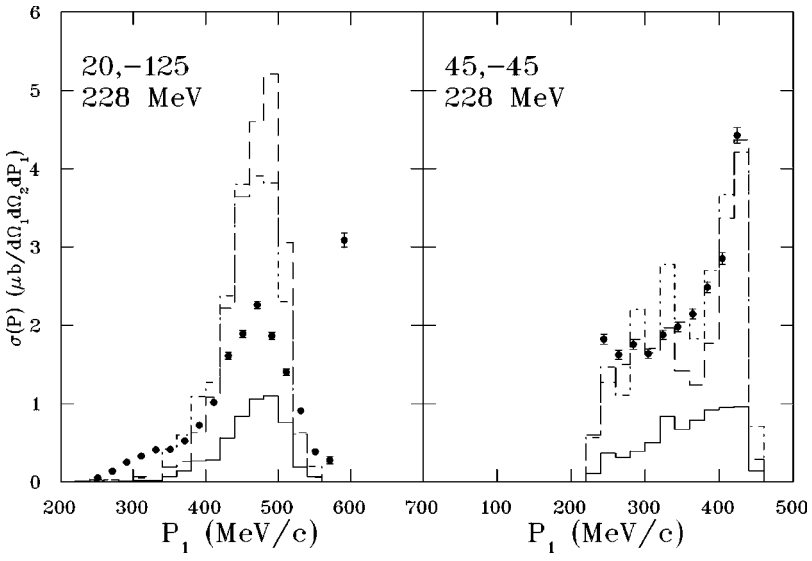

FIG. 8. Double scattering comparing classical (dashed line), fully quantum (solid line), and partial quantum effects without the coherent deuteron wave function (dash-dotted line) at 228 MeV.

$$M = \langle pp| \sum_{i\neq j,j=1,2} e^{i(\mathbf{k}_\pi\cdot\mathbf{r}_j - \mathbf{k}'_\pi\cdot\mathbf{r}_i)} \times \int d\mathbf{q} \frac{f_i(\mathbf{q},\mathbf{k}'_\pi) f_j(\mathbf{k}_\pi,\mathbf{q}) e^{i\mathbf{q}\cdot(\mathbf{r}_i-\mathbf{r}_j)}}{\mathbf{q}^2-\kappa^2} |D\rangle, \quad (17)$$

where the operators f_i are the pion-nucleon amplitudes in spin and isospin space and the bras and kets refer to isospin states only. We have included the initial and final spatial states of the pion but not the final state of the two protons. Since there are two orders of scattering possible and there are two terms in the isospin expansion of the deuteron wave function, there are four terms in this expression, each of the type presented in the previous section.

Thus, since an operator cannot act on the same particle successively the effect of one term on the isospin part of the deuteron wave function is

$$\langle p_1|\langle p_2|(f_2 f_1 + f_1 f_2)\frac{1}{\sqrt{2}}(|p_1\rangle|n_2\rangle - |n_1\rangle|p_2\rangle), \quad (18)$$

where each product of f's can be decomposed into terms from Eq. (16) consisting of a constant multiplying an operator. We make the simplifying approximation that the amplitudes for the elastic scatterings and charge exchanges depend only on the pion momentum (neglecting the nucleon motion). Thus, we assume all nucleons at rest for the purpose of the evaluation of the πN amplitudes only.

These considerations allow us to write this in the form

$$f_2^x(k'_\pi)f_1^+(k_\pi) - f_2^0(k'_\pi)f_1^x(k_\pi) + f_1^0(k'_\pi)f_2^x(k_\pi) - f_1^x(k'_\pi)f_2^+(k_\pi), \quad (19)$$

where f_i^x, f_i^0, and f_i^+ are, respectively, charge exchange, π^0 scattering, and π^+ scattering on nucleon i.

Considering, term by term, the components in Eq. (16) that have the form of constants times operators and taking the expression for double scattering of a generic operator to be represented by $R(\mathbf{r},\mathbf{k}_\pi,\mathbf{k}'_\pi,q_i)$ [$=R(\mathbf{r},q_i)$, suppressing the pion momenta for brevity] and a generic constant amplitude for the corresponding term to be D we can write

$$\begin{aligned}&[D^x(k'_\pi)D^+(k_\pi) - D^0(k'_\pi)D^x(k_\pi)]R(\mathbf{r},q_1)e^{i(\mathbf{k}_\pi+\mathbf{k}'_\pi)\cdot\mathbf{r}/2}\\ &\quad + [D^0(k'_\pi)D^x(k_\pi) - D^x(k'_\pi)D^+(k_\pi)]R(-\mathbf{r},q_2)e^{-i(\mathbf{k}_\pi+\mathbf{k}'_\pi)\cdot\mathbf{r}/2}\\ &\quad = [D^x(k'_\pi)D^+(k_\pi) - D^0(k'_\pi)D^x(k_\pi)][R(\mathbf{r},q_1)e^{i(\mathbf{k}_\pi+\mathbf{k}'_\pi)\cdot\mathbf{r}/2}\\ &\qquad - R(-\mathbf{r},q_2)e^{-i(\mathbf{k}_\pi+\mathbf{k}'_\pi)\cdot\mathbf{r}/2}], \quad (20)\end{aligned}$$

where $\mathbf{q}_i=\mathbf{k}_\pi-\mathbf{k}_i$ is the intermediate momentum of the propagating pion (the same as κ in the previous development) in each case. For example, for the second term in Eq. (16) $D=-iA_1B_2$ and $R=\mathbf{k}'\cdot\hat{\mathbf{r}}g'(r)$.

The subtraction of the strength of the two possible interactions represented by the differences of the multiplying constants D does not depend on the spatial coordinates. The minus sign can be traced to the isospin character of the deuteron.

C. Phases from the proton-proton final state

For the spatial final state wave function of the two protons we have

$$e^{-i(\mathbf{k}_1\cdot\mathbf{r}_1+\mathbf{k}_2\cdot\mathbf{r}_2)} \pm e^{-i(\mathbf{k}_1\cdot\mathbf{r}_2+\mathbf{k}_2\cdot\mathbf{r}_1)} \rightarrow e^{i(\mathbf{k}_2-\mathbf{k}_1)\cdot\mathbf{r}/2} \pm e^{-i(\mathbf{k}_2-\mathbf{k}_1)\cdot\mathbf{r}/2} \quad (21)$$

where the plus sign corresponds to a singlet final state and the minus sign to the triplet final state.

Taking into account the conservation of momentum $\mathbf{k}_\pi = \mathbf{k}'_\pi+\mathbf{k}_1+\mathbf{k}_2$ we can combine the phase factor of the two terms in Eq. (20) (dropping the overall multiplying constant for the moment) to find

$$[e^{i\mathbf{r}\cdot\mathbf{q}_1} \pm e^{i\mathbf{r}\cdot\mathbf{q}_2}]R(\mathbf{r},q_1) - [e^{-i\mathbf{r}\cdot\mathbf{q}_1} \pm e^{-i\mathbf{r}\cdot\mathbf{q}_2}]R(-\mathbf{r},q_2). \quad (22)$$

The operators in Eq. (16) have a definite character in the parity of $\mathbf{r}$, either even or odd. The next step in computing

the quantum matrix element would be to integrate over this vector, thus picking out the matching terms in the final state nucleon wave function. Since we are "correcting" for the quantum effect event by event (and each event has a definite value of $\mathbf{r}$) we cannot proceed to this integration step but we will keep only those terms that would survive this integration. This leads us to the following array which must be applied term by term:

Spin	Triplet to triplet	Triplet to singlet
Even	$[\cos(\mathbf{r}\cdot\mathbf{q}_1)-\cos(\mathbf{r}\cdot\mathbf{q}_2)][R(\mathbf{r},q_1)+R(\mathbf{r},q_2)]$	$[\cos(\mathbf{r}\cdot\mathbf{q}_1)+\cos(\mathbf{r}\cdot\mathbf{q}_2)][R(\mathbf{r},q_1)-R(\mathbf{r},q_2)]$
Odd	$i[\sin(\mathbf{r}\cdot\mathbf{q}_1)-\sin(\mathbf{r}\cdot\mathbf{q}_2)][R(\mathbf{r},q_1)+R(\mathbf{r},q_2)]$	$i[\sin(\mathbf{r}\cdot\mathbf{q}_1)+\sin(\mathbf{r}\cdot\mathbf{q}_2)][R(\mathbf{r},q_1)-R(\mathbf{r},q_2)]$

VI. RESULTS

Calculations were performed (with 4×10^8 cascades) with the quantum effects on double scattering discussed being implemented in the calculation by computing a weight corresponding to each event.

Figure 8 illustrates, for a typical pair of angles, that the isospin correction is the most important quantum effect. The phase correction is much smaller. The constants D in Eq. (20) tend to cancel for the most important partial waves. If the amplitude were completely dominated by the 33 resonance, there would be a constant reduction factor. That dominance is not as pronounced at these energies as at the resonance but there is still a significant cancellation in many cases.

Figures 9 and 10 show the various orders of multiple scattering beyond single. The interactions in the cascade were stopped at fourth order so that quadruple scattering really includes all higher orders which would have occurred if allowed to continue. We have seen that the higher orders of multiple scattering are more important at 294 MeV than at 228 MeV. One possible reason for this is that the absorption is less at the higher energy. When the energy is degraded by collisions, the absorption becomes larger and truncates the multiple scattering. This may be one reason why we have so much multiple scattering.

Figures 11 and 12 give the results for all angular pairs with and without quantum corrections in the double scattering. We have seen that the quantum effects included (especially the isospin one) give a large decrease in the double scattering cross section which carries over into the total as well. We see that the agreement with the data at 228 MeV is generally good with the possible exception of the counter pairs $(60°,-45°)$ and $(60°,-60°)$ where the cross section is overestimated in the midmomentum range. At 294 MeV the agreement is excellent except for a substantial overestimate for the pairs $(60°,-60°)$ and $(20°,-125°)$. Much, but not all, of the overestimate (in the first counter pair at least) can be attributed to third and higher order scatterings which suggests that in some cases the model overestimates these contributions. One possible reason could be that the quantum corrections have not been made to these orders. We anticipate that such corrections would go again in the direction of reducing the cross section but their inclusion, though possible, is beyond the scope of the present work.

The comparison for the counter pair $(125°,-20°)$ at 228 MeV is puzzling. The data reverse their trend from the same pair at 294 MeV while the calculation gives the same general form.

VII. DISCUSSION

The poor agreement of the obtained potential with a semirealistic nucleon-nucleon potential may worry some, and with good reason. However, it seems to be necessary in order to obtain some even more important conditions in a classical simulation. First, the density distribution of nucleons must be correct or else the magnitude of the cross section and estimates of multiple scattering will be wrong. Even the early INC codes did this (more or less) correctly. Second, Fermi momentum must be included. Without this physical effect the coincidence spectra would appear as a series of spikes. The correct degree of smearing is very important. Third, energy must be conserved and definite. If one simply includes the motion of the nucleons without adding a potential to compensate the kinetic energy of the nucleons that corresponds to the Fermi motion, the deuterium nucleus will not have a definite energy and such features as the Jacobian peaks would be washed out. Thus, these three conditions are absolutely essential for the present calculation. The selection of any two implies the third, so there is no choice: we are left with a specified potential.

The nonrealistic nature of this potential mainly affects the single scattering through distortion of the distribution of the final state momentum of the spectator particle. Since single scattering is largely eliminated by the momentum thresholds, we do not expect a large problem. In those cases in which there remains a significant contribution from single scattering, errors may occur. We believe that we have taken the correct compromise for this particular set of observables. For another case (one in which very low energy protons were detected, for example) it might be more appropriate to choose a realistic potential at the expense of the Fermi momentum distribution or the correct density.

The effect of the low-energy experimental cuts is quite important. The single scattering is very large in some cases

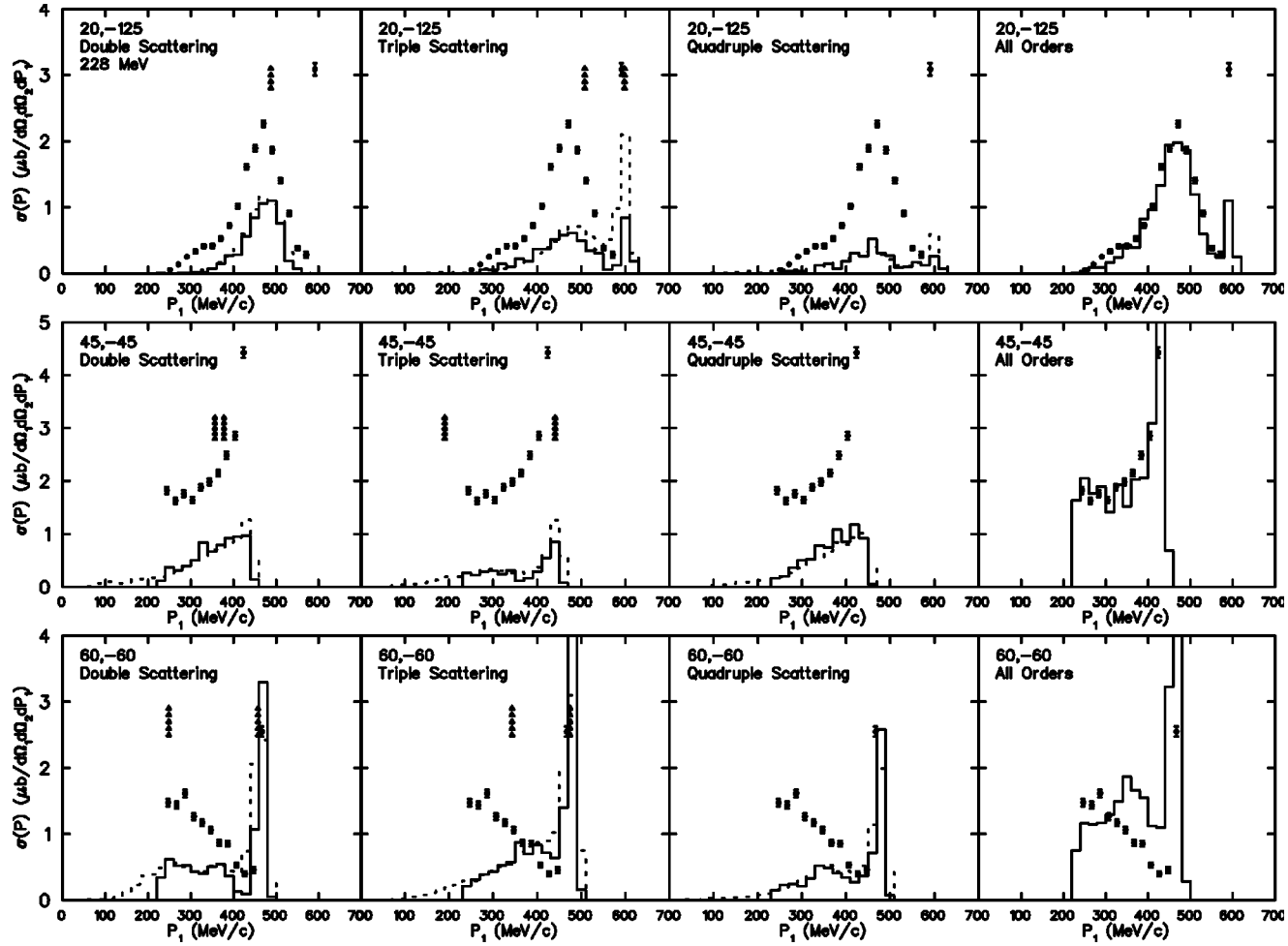

FIG. 9. Comparison of orders of multiple scattering and the total at 228 MeV. The single scattering for $(45°,-45°)$ is shown in Fig. 4.

and small errors in the cuts, which largely eliminate the single scattering, can have a large influence.

In the experimental paper [13] a calculation was presented based on Faddeev equations. Although it is difficult to compare our calculation with that one because the cuts were not taken into account, it seems that we have a better agreement with the data.

This work points out that it is very important to have the correct isospin in the initial state. This can be expected to be most important in the very light elements.

The quantum phase effect seems to be moderate to small. In the original INC it was assumed that the large number of unobserved particles would "wash out" the phases with averaging. It is somewhat surprising that even for this case, with only two nucleons and complete kinematics, this effect is still not very important. Of course, we can make that statement only about the angles tested.

There is some hope that the overestimate of the cross section in the third and fourth orders will be corrected by the introduction of quantum effects in these orders as happened in the second order. The testing of this conjecture is left for future work.

While we began the paper with a very brief review of the beginning history of the INC based on heavy targets and many particles, we have found that a classical simulation (suitably corrected for quantum effects) can be successful in describing even very small systems. To our knowledge this is the first work to try this approach on the deuteron.

ACKNOWLEDGMENTS

We thank R. Tacik for supplying us with tables of data in electronic form. J.P.D. wishes to thank the Department of Physics of New Mexico State University for its hospitality and partial support and W.R.G. expresses appreciation for the same to the Université Paris 7–Denis Diderot. This work was supported by the National Science Foundation under Contract No. PHY-0099729.

APPENDIX A: A SIMPLE LIMIT

In the case where the momentum is determined by a potential, as in the present model, we can get some feeling for this correction (independent of the form of the potential) by considering a simplified case. We assume that particle 2 (the spectator particle) has a given Fermi momentum $\mathbf{p}_2$ with the angle being given by the coincidence counter. Then particle one must have an initial momentum equal and opposite.

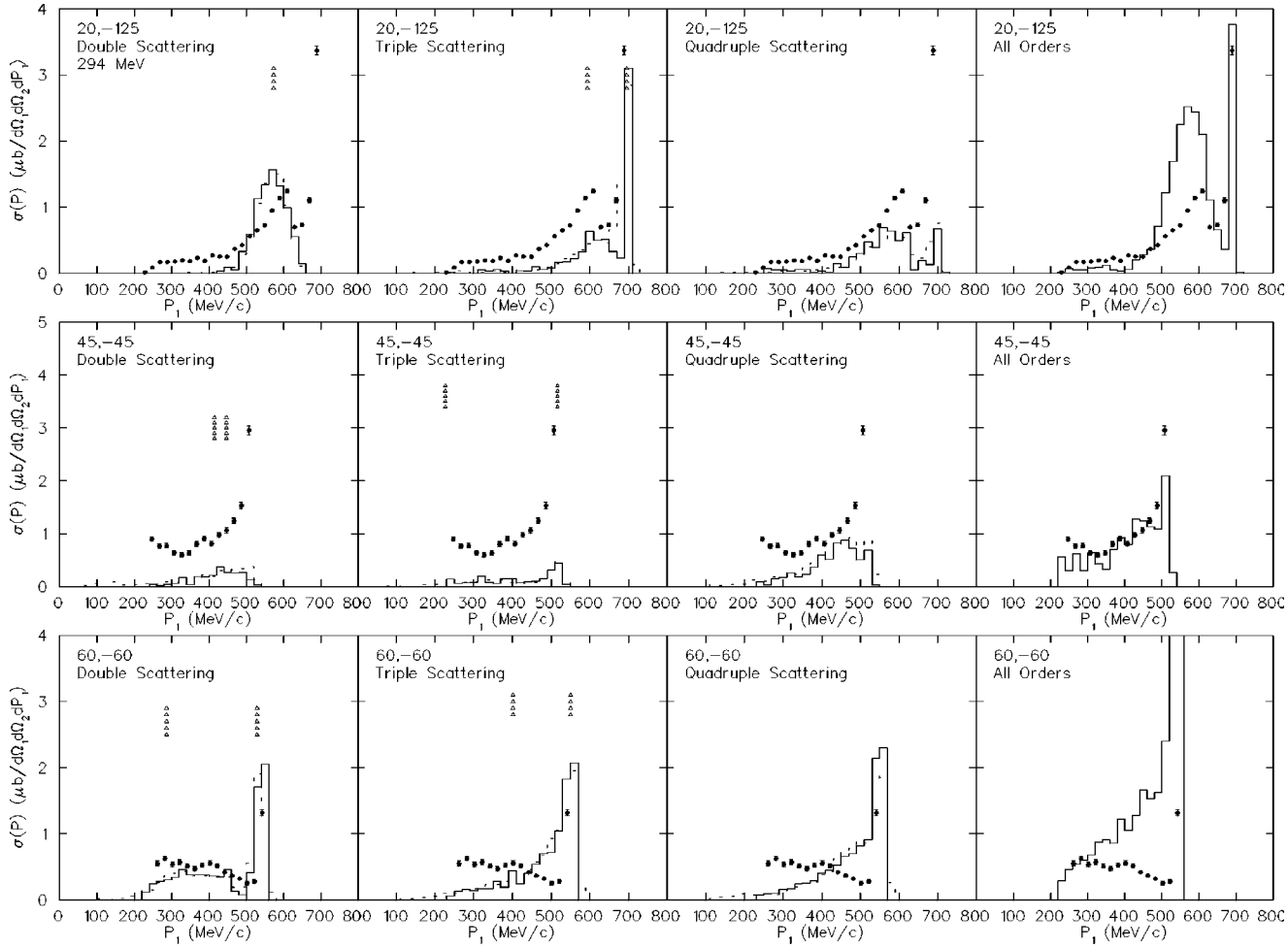

FIG. 10. Comparison of orders of multiple scattering and the total at 294 MeV. The single scattering for $(45°,-45°)$ is shown in Fig. 4.

With the usual center of mass expressions

$$\mathbf{p}=\frac{\mathbf{p}_1-\mathbf{p}_2}{2},\ \ \mathbf{P}=\mathbf{p}_1+\mathbf{p}_2,\ \ \mathbf{p}_1=\frac{\mathbf{P}}{2}+\mathbf{p},\ \ \mathbf{p}_2=\frac{\mathbf{P}}{2}-\mathbf{p}, \tag{A1}$$

where, in fact, $\mathbf{P}=\mathbf{0}$ in this case, we can write the sum of the kinetic and potential energies in the initial state as

$$\frac{\mathbf{p}^2}{m}+V=0, \tag{A2}$$

where we assume zero binding. After the scattering with momentum transfer $\mathbf{q}$, we have

$$\mathbf{p}_2'=\mathbf{p}_2,\ \ \mathbf{p}_1'=\mathbf{p}_1+\mathbf{q},\ \ \mathbf{p}'=\mathbf{p}+\frac{\mathbf{q}}{2}. \tag{A3}$$

In the final state the relative momentum at infinity will be given by

$$\frac{\mathbf{p}_\infty'^2}{m}=\frac{\mathbf{p}'^2}{m}+V=\frac{\mathbf{p}'^2}{m}-\frac{\mathbf{p}^2}{m}\ \text{ or }\ \mathbf{p}_\infty'^2=\mathbf{p}'^2-\mathbf{p}^2=\frac{\mathbf{q}^2}{4}+\mathbf{q}\cdot\mathbf{p}. \tag{A4}$$

Assuming that the direction in the center of mass does not change as the particles propagate to infinity (as would be the case when they are back to back)

$$\mathbf{p}_\infty'=\sqrt{\frac{\mathbf{q}^2}{4}+\mathbf{q}\cdot\mathbf{p}}\frac{\mathbf{p}'}{|\mathbf{p}'|}=\frac{\sqrt{\mathbf{q}^2/4+\mathbf{q}\cdot\mathbf{p}}}{\sqrt{\mathbf{q}^2/4+\mathbf{q}\cdot\mathbf{p}+\mathbf{p}^2}}\left(\mathbf{p}+\frac{\mathbf{q}}{2}\right), \tag{A5}$$

the final momentum of the spectator particle in the laboratory will be

$$\mathbf{p}_{2\infty}'=\frac{\mathbf{q}}{2}+\frac{\sqrt{\mathbf{q}^2/4+\mathbf{q}\cdot\mathbf{p}}}{\sqrt{\mathbf{q}^2/4+\mathbf{q}\cdot\mathbf{p}+\mathbf{p}^2}}\left(\mathbf{p}_2-\frac{\mathbf{q}}{2}\right). \tag{A6}$$

Thus, as $|\mathbf{q}|\to\infty$ the momentum of the spectator in the final state becomes equal to the initial Fermi momentum. However, the present case treats only moderate values of momentum transfer so a substantial correction is to be expected.

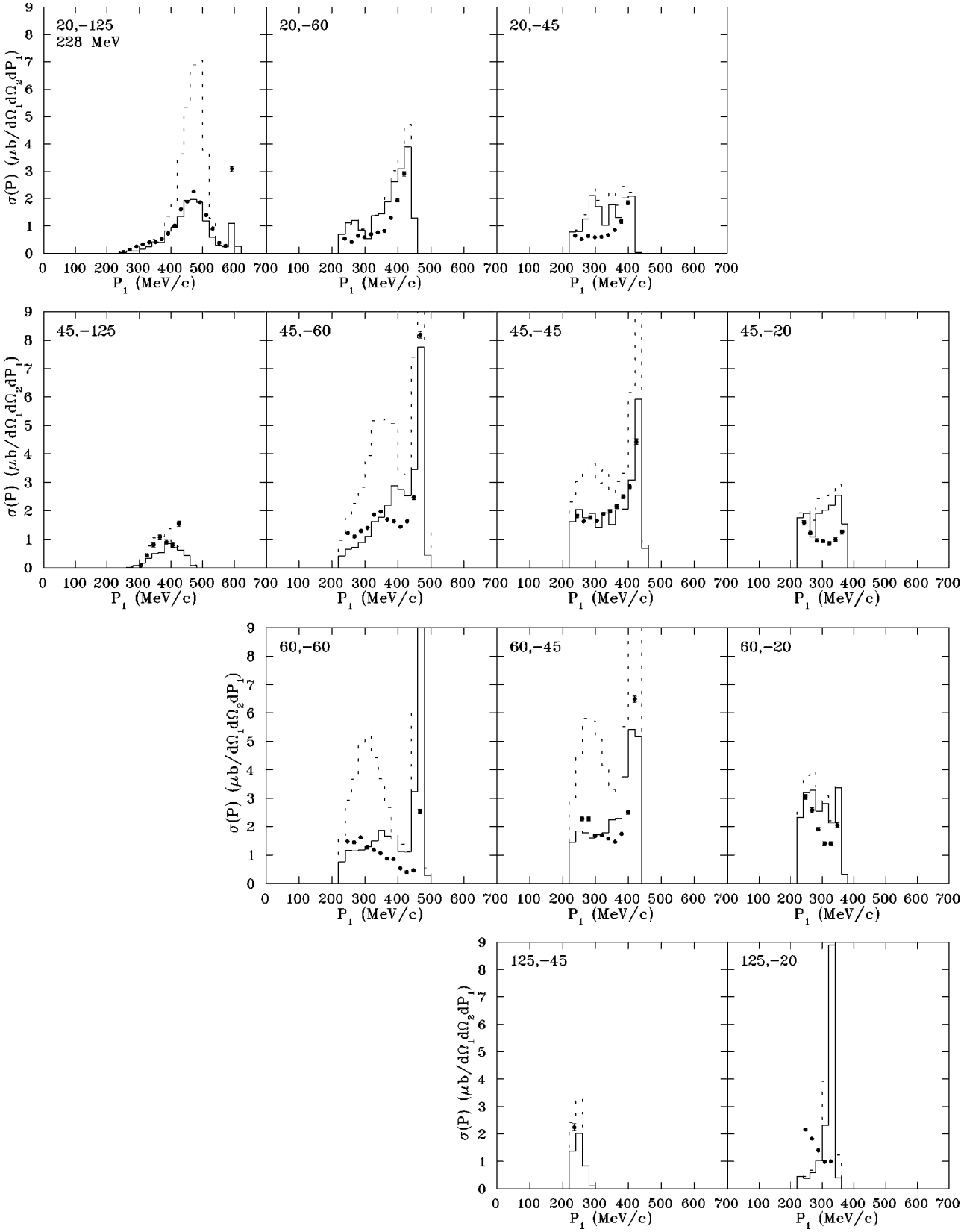

FIG. 11. Total scattering at 228 MeV with (solid) and without (dashed) quantum corrections.

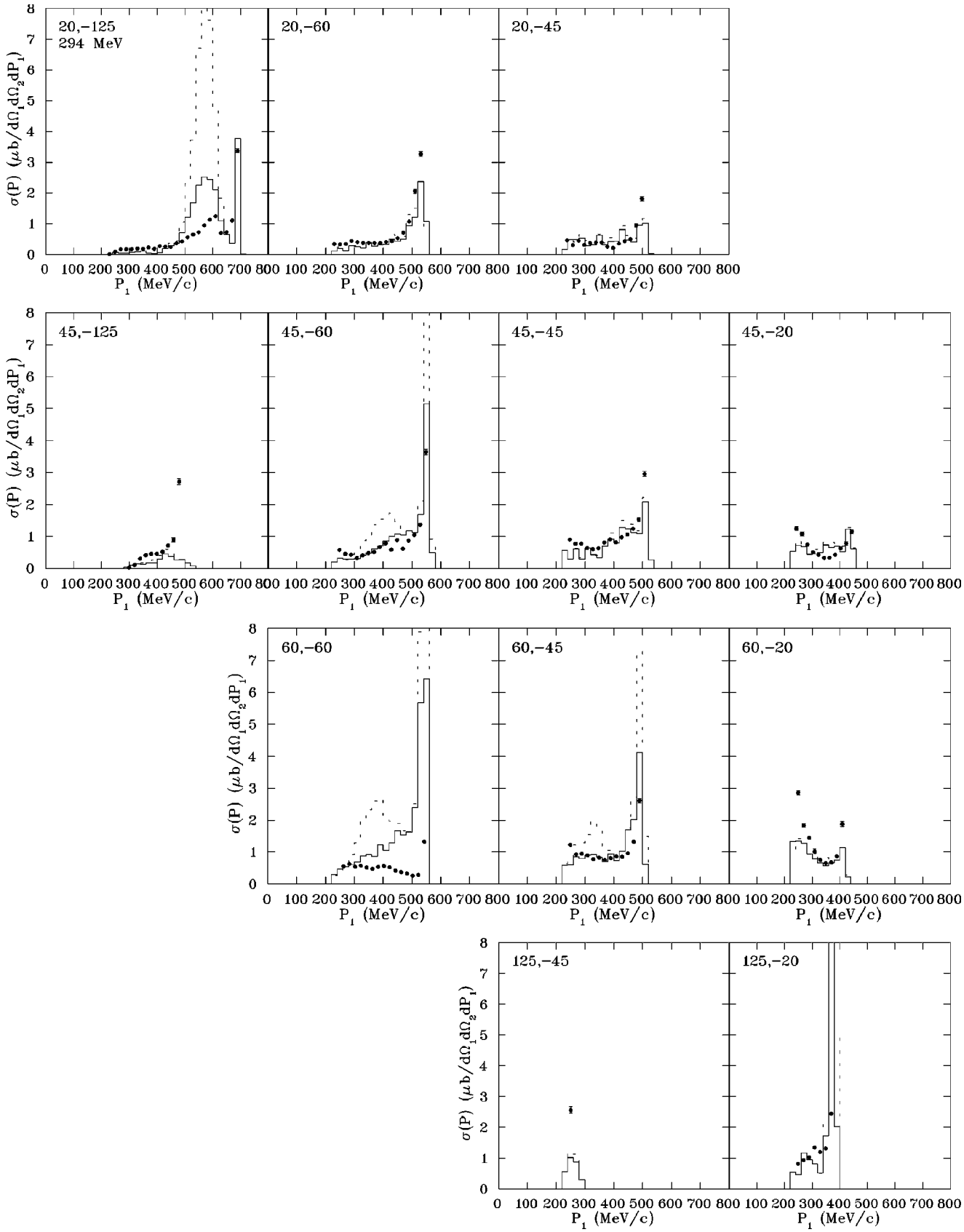

FIG. 12. Total scattering at 294 MeV with (solid) and without (dashed) quantum corrections.

APPENDIX B: SPIN MATRIX ELEMENTS

With the definitions

$$\mathbf{c} = \mathbf{a} \times \mathbf{b}, \tag{B1}$$

$$a^0 = a^z, \quad a^{+1} = \frac{1}{\sqrt{2}}(a^x + ia^y), \quad a^{-1} = -\frac{1}{\sqrt{2}}(a^x - ia^y), \tag{B2}$$

the matrix elements of $\langle S'S'_z|\sigma_1 \cdot \mathbf{a}\sigma_2 \cdot \mathbf{b}|SS_z\rangle$ can be written

		(0,0)	(1,−1)	(1,0)	(1,+1)	(S',S'_z)
(S,S_z)	(0,0)	$-\mathbf{a}\cdot\mathbf{b}$	$-ic^{-1}$	ic^0	$-ic^{+1}$	
	(1,−1)	$-ic^{+1}$	a^0b^0	$-a^0b^{+1}-a^{+1}b^0$	$2a^{+1}b^{+1}$	
	(1,0)	$-ic^0$	$a^0b^{-1}+a^{-1}b^0$	$\mathbf{a}\cdot\mathbf{b}-2a^0b^0$	$a^{+1}b^0+a^0b^{+1}$	
	(1,+1)	$-ic^{-1}$	$2a^{-1}b^{-1}$	$-a^{-1}b^0-a^0b^{-1}$	a^0b^0	

We need this matrix twice, once for $\mathbf{a}=\mathbf{k}$, $\mathbf{b}=\mathbf{k}'$ and once for $\mathbf{a}=\hat{\mathbf{r}}\times\mathbf{k}$, . For the second case we can write $\mathbf{c}=-(\hat{\mathbf{r}}\cdot\mathbf{k}\times\mathbf{k}')\hat{\mathbf{r}}$.

For a single spin operator we have

	(0,0)	(1,−1)	(1,0)	(1,+1)
(0,0)	0	$-a^{-1}$	a^0	$-a^{+1}$
(1,−1)	a^{+1}	$-a^0$	a^{+1}	0
(1,0)	a^0	$-a^{-1}$	0	a^{+1}
(1,+1)	a^{-1}	0	$-a^{-1}$	a^0

for the matrix elements of $\langle S'S'_z|\sigma_1 \cdot \mathbf{a}|SS_z\rangle$ and

	(0,0)	(1,−1)	(1,0)	(1,+1)
(0,0)	0	$+a^{-1}$	$-a^0$	a^{+1}
(1,−1)	$-a^{+1}$	$-a^0$	a^{+1}	0
(1,0)	$-a^0$	$-a^{-1}$	0	a^{+1}
(1,+1)	$-a^{-1}$	0	$-a^{-1}$	a^0

for the matrix elements of $\langle S'S'_z|\sigma_2 \cdot \mathbf{a}|SS_z\rangle$.

[1] R. Serber, Phys. Rev. **72**, 1114 (1947).
[2] M. L. Goldberger, Phys. Rev. **74**, 1268 (1948).
[3] G. Bernardini, E. T. Booth, and S. J. Lindenbaum, Phys. Rev. **85**, 826 (1952); **88**, 1017 (1952).
[4] N. Metropolis, R. Bivins, M. Storm, A. Turkevich, J. M. Miller, and G. Friedlander, Phys. Rev. **110**, 185 (1958).
[5] N. Metropolis, R. Bivins, M. Storm, J. M. Miller, G. Friedlander, and A. Turkevich, Phys. Rev. **110**, 204 (1958).
[6] J. N. Ginocchio, Phys. Rev. C **17**, 195 (1978).
[7] Y. Yariv and A. Frankel, Phys. Rev. C **20**, 2227 (1979).
[8] R. Mattiello, H. Sorge, H. Stöcker, and W. Greiner, Phys. Rev. Lett. **63**, 1459 (1989); H. Sorge, R. Mattiello, H. Stöcker, and W. Greiner, *ibid.* **68**, 286 (1992).
[9] J. Cugnon, Phys. Rev. C **22**, 1885 (1980); G. Montarou *et al.*, *ibid.* **47**, 2764 (1993); J. Cugnon, *ibid.* **23**, 2094 (1981); J. Cugnon, D. Kinet, and J. Vandermeulen, Nucl. Phys. **A379**, 553 (1982); M. Cahay, J. Cugnon, and J. Vandermeulen, *ibid.* **A393**, 237 (1983).
[10] L. L. Salcedo, E. Oset, M. J. Vicente-Vacas, and C. Garcia-Recio, Nucl. Phys. **A484**, 557 (1988); B. M. Abramov *et al.*, Phys. At. Nucl. **59**, 376 (1996); M. J. Vicente, E. Oset, L. L. Salcedo, and C. Garcia-Recio, Phys. Rev. C **39**, 209 (1989).
[11] B. Li and W. Bauer, Phys. Rev. C **44**, 450 (1991); B. Li, W. Bauer, and C. M. Ko, Phys. Lett. B **382**, 337 (1996).
[12] S. H. Kahana, D. E. Kahana, Y. Pang, and T. J. Schlagel, Annu. Rev. Nucl. Part. Sci. **46**, 31 (1996).
[13] R. Tacik, E. T. Boschitz, W. Gyles, C. R. Ottermann, M. Wessler, U. Wiedner, H. Garcilazo, and R. R. Johnson, Phys. Rev. C **42**, 1846 (1990).
[14] D. Strottman and W. R. Gibbs, Phys. Lett. **149B**, 288 (1984).
[15] W. R. Gibbs, in *Intersections Between Particle and Nuclear Physics*, edited by D. F. Geesaman, AIP Conf. Proc. No. 150 (AIP, New York, 1986), p. 505.
[16] W. R. Gibbs and D. Strottman, in *Proceedings of the International Conference on Antinucleon- and Nucleon-Nucleon Interactions, Telluride, CO*, edited by G. E. Walker, C. D. Goodman, and C. Olmer (Plenum, New York, 1985), p. 381 ff.
[17] W. R. Gibbs, in Proceedings of the First Fermilab Workshop on Antimatter Physics at Low Energy, edited by B. E. Bonner and L. S. Pinsky, Fermilab, Batavia, IL, 1986.
[18] W. R. Gibbs and J. W. Kruk, Phys. Lett. B **317**, 237 (1990); Z. Phys. C **46**, S45 (1990).
[19] W. R. Gibbs and W. B. Kaufmann, in Proceedings of the Workshop on Physics with Light Mesons, 1987, Report No. LA-11184-C, 1987, p. 28.
[20] S. Ahmad *et al.*, *Proceedings of the Fourth Biennial Confer-*

ence on Low Energy Antiproton Physics, Dinkelsbühl, Germany, 1996 [Nucl. Phys. B (Proc. Suppl.) **56A**, 118 (1997)].
[21] W. R. Gibbs and W. B. Kaufmann, in *Pion-Nucleus Physics: Future Directions and New Facilities at LAMPF*, edited by R. J. Peterson and D. D. Strottman, AIP Conf. Proc. No. 163 (AIP, New York, 1988), p. 279.
[22] J. D. Zumbro, C. L. Morris, J. A. McGill, S. J. Seestrom, R. M. Whitton, C. M. Riedel-Edwards, A. L. Williams, M. Braunstein, M. Kohler, B. Kriss, S. Hoibraten, R. J. Peterson, J. Ouyang, J. E. Wise, and W. R. Gibbs, Phys. Rev. Lett. **71**, 1796 (1993).
[23] M. Alqadi and W. R. Gibbs, Phys. Rev. C **65**, 044609 (2002).
[24] B. G. Ritchie, Phys. Rev. C **28**, 926 (1983).
[25] T. E. O. Ericson and M. Rosa-Clot, Nucl. Phys. **A405**, 497 (1983).
[26] J. L. Friar, B. F. Gibson, and G. L. Payne, Phys. Rev. C **30**, 1084 (1984).
[27] J. L. Ballot and M. R. Robilotta, Phys. Rev. C **45**, 986 (1992); **45**, 990 (1992);J. L. Ballot, A. M. Eiró, and M. R. Robilotta, *ibid.* **40**, 1459 (1989).
[28] W. R. Gibbs, *Computation in Modern Physics* (World Scientific, Singapore, 1994).
[29] M. Bernheim, A. Bussière, J. Mougey, D. Royer, D. Tarnowski, S. Turck-Chièze, G. P. Capitani, E. Desanctis, and E. Jans, Nucl. Phys. **A365**, 349 (1981).
[30] R. A. Malfliet and J. A. Tjon, Nucl. Phys. **A127**, 161 (1969).
[31] W. R. Gibbs, M. Elghossain, and W. B. Kaufmann, Phys. Rev. C **48**, 1546 (1993).